Available online at www.sciencedirect.com

ScienceDirect

Ceramics International 37 (2011) 1859–1864

CERAMICS INTERNATIONAL

www.elsevier.com/locate/ceramint

Fabrication of $BaTiO_3$-PTFE composite film for embedded capacitor employing aerosol deposition

Yoon-Hyun Kim [a], Hyung-Jun Kim [a], Jung-Hyuk Koh [a], Jae-Geun Ha [a], Young-Hoon Yun [b], Song-Min Nam [a,*]

[a] Department of Electronic Materials Engineering, Kwangwoon University 447-1, Wolgye-dong, Nowon-gu, Seoul 139-701, Republic of Korea
[b] Department of Hydrogen & Fuel Cell Tech., Dongshin University, 253, Geonjae-ro, Naju-si, Jeonnam 520-714, Republic of Korea

Received 29 November 2010; received in revised form 20 December 2010; accepted 6 February 2011
Available online 29 March 2011

Abstract

The potential for using aerosol deposition (AD) as an alternative fabrication method to the conventional polymer composite process for embedded capacitors was examined. In order to achieve a high relative dielectric permittivity, $BaTiO_3$-polytetrafluoroethylene (PTFE) composite thick films were attempted by AD at room temperature. For the high dielectric constant, the $BaTiO_3$-PTFE composite films grown by AD should satisfied the following two critical conditions: a reduced decrement in ceramic particle size and a relieved distortion of the crystal structure. However, the relative permitivity of the composite films was too low compared with that of the $BaTiO_3$ films grown by AD. By predicting the dielectric constant in several composite models using the Hashin–Shtrikman bounds theory and 3-dimenstional (3-D) electrostatic simulation, we confirmed that the connectivity between ceramic particles is a highly critical factor for achieving a high dielectric constant in composite films.

Keywords: B. Composite; C. Dielectric properties; D. $BaTiO_3$ and titanates; Aerosol deposition (AD)

1. Introduction

With the digital convergence of information technology, telecommunication, consumer electronics, and entertainment, research and development is focusing on the 3-dimenstional (3-D) integrations of electronic components by means of embedded planar technologies. Especially, the widely used decoupling capacitors must be changed from surface mount technologies to embedded planar technologies due to the high-frequency operation and the large occupation percentage of decoupling capacitors in today's electronic devices [1]. The fabrication of such embedded planar decoupling capacitors requires low-temperature technologies for the development of ceramic materials as such materials generally need high processing temperatures above 1000 °C. In order to overcome this problem, polymer composites have been investigated, but they suffered due to low ceramic contents of below 60 vol.% in the composites and low dielectric constant [2–4].

Our research group has focused on the aerosol deposition (AD) process as a novel, low-temperature process for developing embedded decoupling capacitors with high capacitance density due to its superior merits of room temperature processing, high deposition rate, and high density. However, the relative permittivity of $BaTiO_3$ films aerosol-deposited at room temperature was sharply reduced to approximately 100 from the general range of 1000–3000 that is typical for $BaTiO_3$ powder. This abrupt decrease in their relative permitivity was attributed to the collision impact of particles in the AD process [5,6]. During the AD process, accelerated ceramic particles are ejected through a nozzle and then impacted at a velocity of 200–300 m/s onto a substrate to form nano-sized $BaTiO_3$ films. These particle collision impacts cause crystal lattice distortion, internal stress, and small crystallite size in $BaTiO_3$ films grown by AD.

In our previous research on flexible integrated substrates fabricated by AD, we attempted to fabricate the ceramic-polymer composite thick films by AD to overcome the problems of ceramic materials, such as brittleness and fragileness. Al_2O_3-polymer composite thick films were successfully fabricated by AD and its good dielectric properties

* Corresponding author. Tel.: +82 2 9405764; fax: +82 2 9425764.
E-mail address: smnam@kw.ac.kr (S.-M. Nam).

0272-8842/$36.00 © 2011 Elsevier Ltd and Techna Group S.r.l. All rights reserved.
doi:10.1016/j.ceramint.2011.02.014

were confirmed [7–9]. The decrement of the crystallite size of Al_2O_3 ceramics in Al_2O_3-polymer composite films was reduced due to the cushion-effect of the polymer.

In this paper, this polymer elasticity is used to relieve the collision impact of $BaTiO_3$ particles in the AD process and hence facilitate the fabrication of $BaTiO_3$-PTFE composite films with high dielectric constant. Additionally, several ceramic-polymer composite models are designed and their permittivity is calculated by 3-D electrostatic simulation to confirm the causes of the polymer composite's low dielectric constant.

2. Experimental

The AD process is based on shock loading solidification due to the impact of ultra-fine particles accelerated through a nozzle by carrier gases, as described elsewhere [10,11]. $BaTiO_3$ and $BaTiO_3$-PTFE composite films were prepared by AD by using commercial $BaTiO_3$ powders (BT-04, SAKAI CHEMICAL INDUSTRY CO., Ltd., Japan) with a particle size of 0.45 μm as starting powders. The particles were aerosolized in an aerosol chamber and transported into a deposition chamber by He gas at a flow rate of 7 L/min. The orifice size of the nozzle was 10×0.4 mm^2, the deposition area 10×10 mm^2, the distance between the substrates 10 mm, the working pressure 21 Torr, and the deposition time 1 min 30 s. For the fabrication of the $BaTiO_3$-PTFE composite films by AD, PTFE powders (Daikin POLYFLON L-5 PTFE Low polymer, DAIKIN INDUSTRIES, Ltd., Japan) with a particle size of 0.15 μm and the aforementioned $BaTiO_3$ powders were chosen as starting powders. A $BaTiO_3$-PTFE mixed powder with a PTFE powder content of 0.1 wt.% was prepared, milled with ethanol for 24 h and dried at 80 °C for 48 h. The $BaTiO_3$-PTFE composite films were fabricated at room temperature by AD. The He gas flow rate was 4 L/min, the working pressure 5.5 Torr, and the deposition time 5 min. The other conditions were the same as those of the aerosol-deposited $BaTiO_3$ films. The surface morphologies of the films were observed using a field-emission scanning electron microscopy (FE-SEM, S-4700, HITACHI Ltd., Japan). Next, the crystallinity and crystallite size were analyzed by using an X-ray diffractometer (XRD, X'Pert PRO, PAN alytical). Finally, the dielectric properties of the films were measured using an impedance analyzer (HP 4194A, Agilent). Various simulation models were designed and their permittivity calculated using 3-D electrostatic simulation (ANSYS Ver.12.10, ANSYS, Inc.) in order to confirm the causes of low permittivity in the composite films.

3. Results and discussion

3.1. Microstructures of the $BaTiO_3$ and $BaTiO_3$-PTFE composite films fabricated by AD process

The $BaTiO_3$ and $BaTiO_3$-PTFE composite films were successfully fabricated on Cu and glass substrates by AD. The aerosol-deposited $BaTiO_3$ films were dense without any pores, as shown in Fig. 1(a) and (c). However, the XRD pattern of the $BaTiO_3$ films exhibited a slight peak shift in comparison with that of the as-received $BaTiO_3$ powders, as shown in Fig. 2(a) and (b). The calculated crystallite size of these films according to Scherrer equation was 11.2 nm based on the 110 peak. The distortion of the crystal structure and the internal

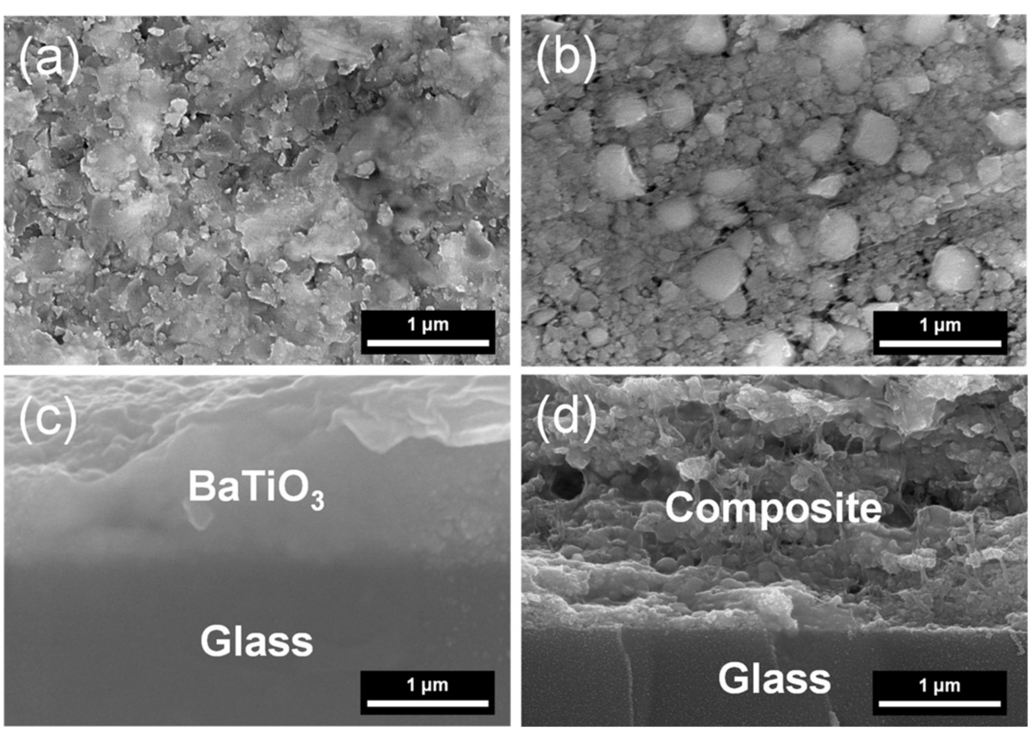

Fig. 1. Surface SEM images of the (a) $BaTiO_3$ and (b) $BaTiO_3$-PTFE composite films and cross-sectional SEM images of the (c) $BaTiO_3$ and (d) $BaTiO_3$-PTFE composite films on glass substrates.

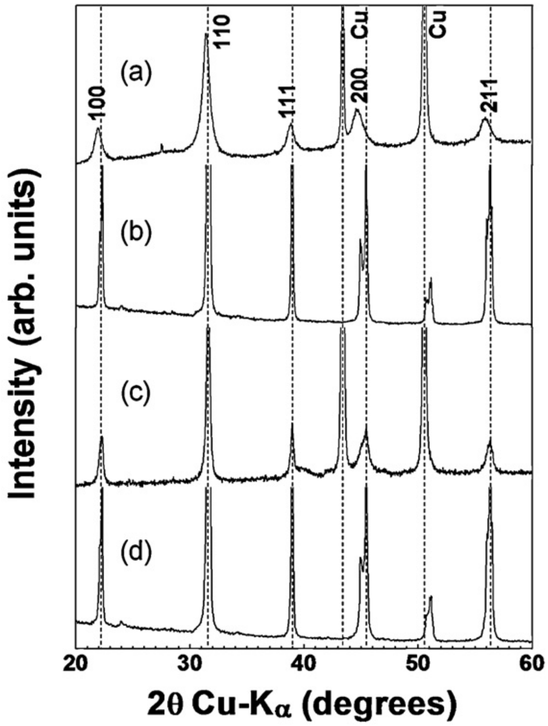

Fig. 2. X-ray diffraction patterns of the (a) $BaTiO_3$ films on Cu substrates, (b) $BaTiO_3$ starting powders, (c) $BaTiO_3$-PTFE composite films on Cu substrates, and (d) $BaTiO_3$-PTFE starting powders.

stress in the $BaTiO_3$ films would be confirmed from the peak shift and small crystallites size. On the other hand, the $BaTiO_3$ particles maintained their particles size in the $BaTiO_3$-PTFE composite films, as shown in Fig. 1(b) and (d), and no peak shift was observed in their XRD pattern in comparison with that of the $BaTiO_3$-PTFE mixing powders, as shown in Fig. 2(c) and (d). The crystallite size of the $BaTiO_3$ material in the $BaTiO_3$-PTFE composite films was calculated as 24.6 nm based on the 110 peak by using Scherrer equation, which was double that of the $BaTiO_3$ films. The crystal structure of the $BaTiO_3$ films was confirmed as cubic phase, as shown in Fig. 3(a). However, the tetragonal phase of the $BaTiO_3$ material was still existed in the $BaTiO_3$-PTFE composite films. Consequently, the decrement in the $BaTiO_3$ particle size was reduced and the distortion of the crystal structures was relieved in the $BaTiO_3$-PTFE composite films owing to the elasticity of the PTFE material. Fig. 4 illustrated the growth of the $BaTiO_3$ and composite films.

3.2. Dielectric properties of the $BaTiO_3$ films and $BaTiO_3$-PTFE composite films

The relative permittivity and loss tangent of the $BaTiO_3$ films were 64 and 0.073 at 100 kHz, respectively, as shown in Fig. 5(a). These values agreed well with those previously reported [5,6]. The equivalent values for the $BaTiO_3$-PTFE composite films were 15 and 0.091, respectively, as shown in Fig. 5(b). However, contrary to the expectations based on the microstructure observations, this relative permittivity was too low compared with that of the $BaTiO_3$ films, which was attributed to the content of the ceramic material and the films' inner structure.

3.3. Calculation of the dielectric constant of the aerosol-deposited $BaTiO_3$-PTFE composite model using 3-D electrostatic simulation

We firstly considered the ceramic content in the composite films as the possible cause of the low permittivity of the aerosol-deposited $BaTiO_3$-PTFE composite films. To investigate the effects of ceramic content on the dielectric constant of the composite films, the top and bottom limits for the dependence of the relative permittivity of the composite films on the ceramic content were plotted using Hashin–Shtrikman bounds theory, as shown in Fig. 6(a) [12]. The relative permittivity of the composite films at certain ceramic content was placed within the range of the top (ε_T) and bottom (ε_B) limits. The top and bottom limits of the composite, consisting of two phases with dielectric constants of ε_1 and ε_2, are expressed by Eqs. (1) and (2), respectively, where d means dimension and V_1 and V_2 are the volume fractions of the two phases 1 and 2, respectively. Eqs. (3) and (4) show the definition of $\langle\varepsilon_a\rangle$ and $\langle\varepsilon_b\rangle$, respectively.

$$\varepsilon_T = \langle\varepsilon_a\rangle - \frac{V_1 V_2(\varepsilon_2 - \varepsilon_1)^2}{\langle\varepsilon_b\rangle + (d-1)\varepsilon_2} \quad (1)$$

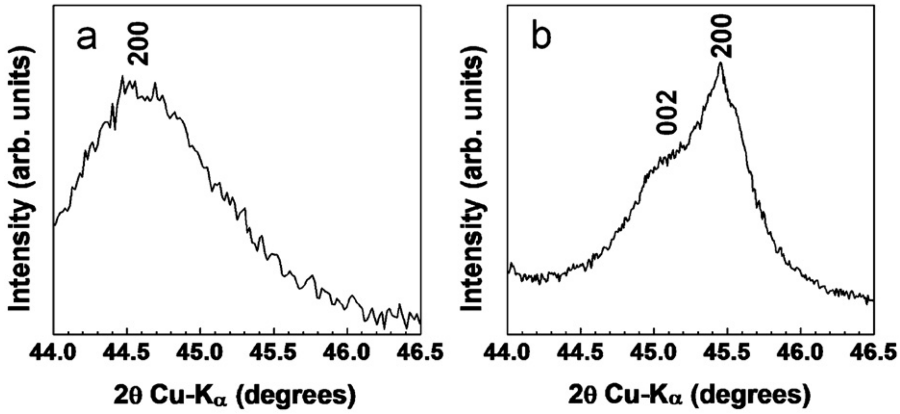

Fig. 3. Enlarged 200 peak of the (a) $BaTiO_3$ and (b) $BaTiO_3$-PTFE composite films fabricated by AD.

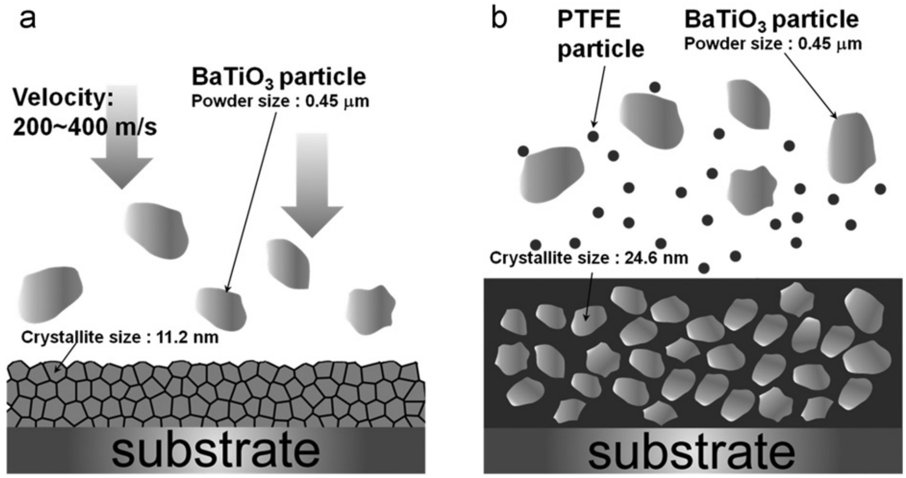

Fig. 4. Schematic diagrams showing the growth of the (a) $BaTiO_3$ and (b) $BaTiO_3$-PTFE composite films fabricated by AD.

$$\varepsilon_B = \langle\varepsilon_a\rangle - \frac{V_1 V_2(\varepsilon_2 - \varepsilon_1)^2}{\langle\varepsilon_b\rangle + (d-1)\varepsilon_1} \tag{2}$$

$$\langle\varepsilon_a\rangle = \varepsilon_1 V_1 + \varepsilon_2 V_2 \tag{3}$$

$$\langle\varepsilon_b\rangle = \varepsilon_1 V_2 + \varepsilon_2 V_1 \tag{4}$$

This result confirmed the large gap between the top and bottom limits of the dielectric constant. A complete explanation of the causes of this large gap will facilitate the development of a method capable of fabricating composite films with high permittivity close to the top limit. We ascribed this large gap to the inner structure of the composite films. Therefore, various simulation models based on the planar capacitor model with the $BaTiO_3$-PTFE composite layer were designed using 3-D electrostatic simulation by considering the connectivity between ceramic particles. Fig. 6(b) and (c) show the designed contact and non-contact models, respectively. Small cubes and empty parts in the models were assigned as the $BaTiO_3$ ($\varepsilon_r = 3000$) and PTFE ($\varepsilon_r = 2.1$) materials, respectively. These small cubes in the contact models were perfectly connected with each other but there was no such connectivity in the non-contact models. The size of the planar capacitor model was 6 μm × 6 μm × 3 μm and the excitation voltage was 1 V.

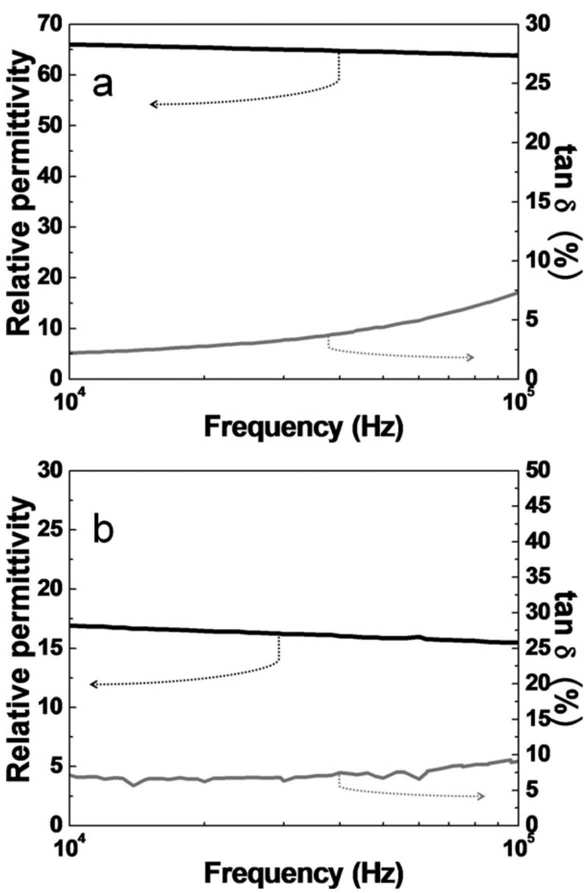

Fig. 5. Frequency dependence of relative permittivity and loss tangent of the (a) $BaTiO_3$ and (b) $BaTiO_3$-PTFE composite films fabricated by AD.

The simulations results confirmed the action of two factors in influencing the dielectric constant of the composite films. Firstly, the dielectric constant of the contact models was increased with increasing $BaTiO_3$ content following the ε_T of the Hashin–Shtrikman bounds, as shown in Fig. 6(a). Secondly, the large gap between ε_T and ε_B resulted from the connectivity between the $BaTiO_3$ particles. Although the contact model (Fig. 6(b)) with 60.2 vol.% and the non-contact model (Fig. 6(c)) with 60.4 vol% were assigned with approximately the same $BaTiO_3$ content, their relative permittivity differed by over 1000. And also, the relative permittivity calculated for the contact and non-contact models with $BaTiO_3$ contents of 70, 80, and 90 vol.% agreed well with our prediction. Additionally, models with randomly connected $BaTiO_3$ particles were prepared to confirm the relation between ceramic particle connectivity and their dielectric constant, as shown in Fig. 6(a). Their total $BaTiO_3$ content was approximately the same at 80 vol.%. Their connected $BaTiO_3$ volume content was increased from 41.1 to 99.2 vol.%. Fig. 6(d) shows the model with 88.9 vol.% of the $BaTiO_3$ particles randomly connected and 11.1 vol.% separated. This simulation result demonstrated that the increase in the connectivity between the $BaTiO_3$ particles directly affected the increase in the dielectric constant of the composite model, as shown in Fig. 6(a). This confirmed

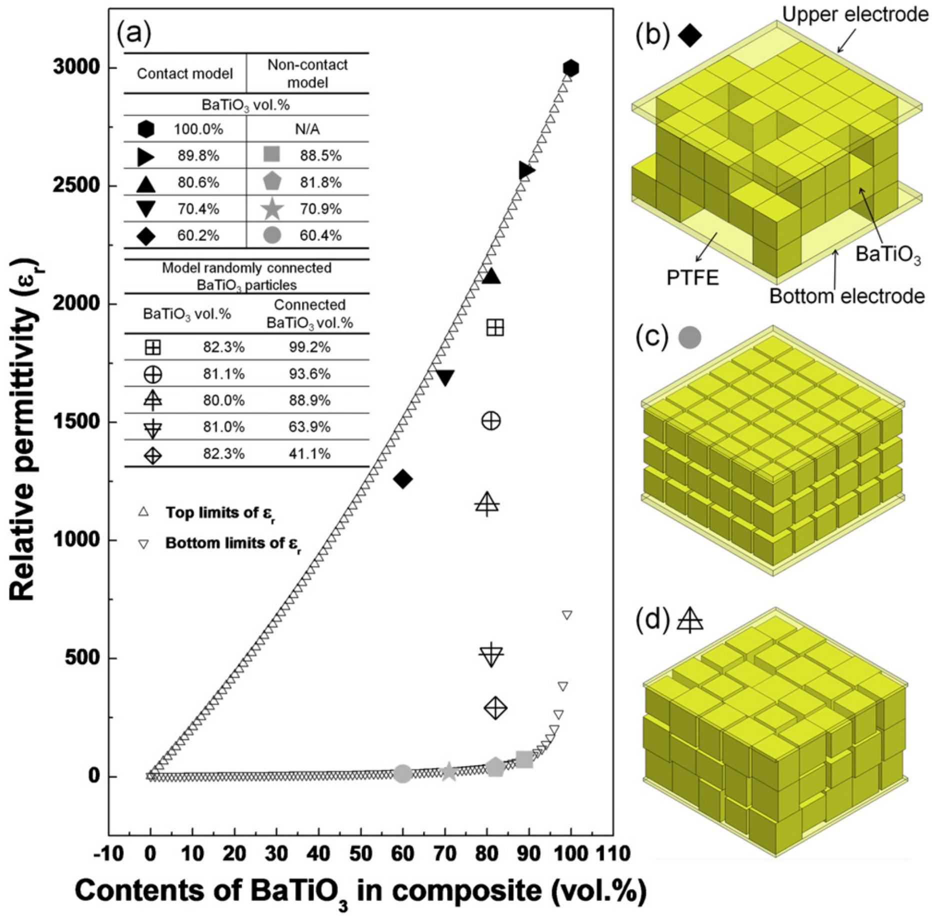

Fig. 6. (a) Hashin–Shtrikman bounds of $BaTiO_3$-PTFE composites model as a function of $BaTiO_3$ content, (b) contact model with a $BaTiO_3$ content of 60.2 vol.%, (c) non-contact models with a $BaTiO_3$ content of 60.4 vol.%, and (d) model with 88.9 vol.% of the $BaTiO_3$ particles randomly connected.

that the connectivity between ceramic particles is a highly critical factor for achieving high permittivity. Achieving such connectivity between ceramic particles in the conventional polymer composite process is very difficult due to the resulting dispersion of the powder in the suspensions. In the AD process, the physical acceleration of the ceramic particles can be used to increase the connectivity between ceramic particles.

4. Conclusions

This article has proposed the AD process as a suitable fabrication method for $BaTiO_3$-PTFE composite films applied to embedded capacitors. The $BaTiO_3$ and $BaTiO_3$-PTFE composite thick films were successfully fabricated by AD at room temperature. The decrement in the $BaTiO_3$ particle size was reduced and the distortion of the crystal structures was relieved in the $BaTiO_3$-PTFE composite films due to the elasticity of the PTFE material. However, the relative permitivity of composite films was too low compared with that of the $BaTiO_3$ films. The prediction of the dielectric constant in the composite models using Hashin–Shtrikman bounds theory and 3-D electrostatic simulation confirmed the critical influence of the connectivity between the ceramic particles in attaining high permittivity in composite films.

Acknowledgements

This work was supported by the Grant of the Korean Ministry of Education, Science and Technology (The Regional Core Research Program/Biohousing Research Institute).

References

[1] Y. Rao, S. Ogitani, P. Kohl, C.P. Wong, Novel polymer–ceramic nanocomposite based on high dielectric constant epoxy formula for embedded capacitor application, J. Appl. Polym. Sci. 83 (2002) 1084–1090.

[2] H. Windlass, P.M. Raj, D. Balaraman, S.K. Bhattacharya, R.R. Tummala, Polymer–ceramic nanocomposite capacitors for system-on-package (SOP) applications, IEEE Transact. Adv. Package 26 (2003) 10–16.

[3] H. Windlass, P.M. Raj, D. Balaraman, S.K. Bhattacharya, R.R. Tummala, Colloidal processing of polymer ceramic nanocomposite integral capacitors, IEEE Transact. Electron. Packaging Manuf. 26 (2003) 100–105.

[4] S.D. Cho, S.Y. Lee, J.G. Hyun, K.W. Paik, Comparison of theoretical predictions and experimental values of the dielectric constant of epoxy/$BaTiO_3$ composite embedded capacitor films, J. Mater. Sci.: Mater. Electron. 16 (2005) 77–84.

[5] H. Hatono, T. Ito, K. Iwata, J. Akedo, Multilayer construction with various ceramic films for electronic devices fabricated by aerosol deposition, Int. J. Appl. Ceram. Technol. 3 (2006) 419–427.

[6] H. Hatono, T. Ito, A. Matsumura, Application of $BaTiO_3$ film deposited by aerosol deposition to decoupling capacitor, Jpn. J. Appl. Phys. 46 (2007) 6915–6919.

[7] H.J. Kim, Y.J. Yoon, J.H. Kim, S.M. Nam, Application of Al_2O_3-based polyimide composite thick films to integrated substrates using aerosol deposition method, Mater. Sci. Eng. B 161 (2009) 104–108.
[8] H.J. Kim, S.M. Nam, Effects of heat treatment on the dielectric properties of aerosol-deposited Al_2O_3-polyimide composite thick films for room-temperature fabrication, J. Ceram. Process. Res. 10 (2009) 817~822.
[9] H.J. Kim, Y.H. Kim, Y.J. Yoon, J.H. Kim, S.M. Nam, Calculation of Al_2O_3 contents in Al_2O_3-PTFE composite thick films fabricated by using the aerosol deposition, J. Korean Phys. Soc. 57 (2010) 1086–1091.
[10] J. Akedo, Room temperature impact consolidation (RTIC) of fine ceramic powder by aerosol deposition method and applications to microdevices, J. Therm. Spray Technol. 17 (2008) 181–198.
[11] J. Akedo, Aerosol deposition of ceramic thick films at room temperature: densification mechanism of ceramic layers, J. Am. Ceram. Soc. 89 (2006) 1834–1839.
[12] S. Torquato, Random Heterogeneous Materials: Microstructure and Macroscopic Properties, Springer, 2002 552–592.